

Inoculated Slightly Hypereutectic Gray Cast Irons

Mihai Chisamera, Iulian Riposan, Stelian Stan, Cristina Militaru, Irina Anton, and Michael Barstow

(Submitted May 27, 2010; in revised form January 29, 2011)

The current experimental investigation in this article was designed to characterize the structure of mold (M) and ladle (L) inoculated, low-S (0.025 wt.% S), low-Al (0.003 wt.% Al), slightly hypereutectic (CE = 4.4–4.5 wt.%) electric melted gray irons, typical for high performance thin-wall castings. It describes the effect of a Ca, Al, Zr-FeSi inoculant addition of 0–0.25 wt.% on structure characteristics, and compares to similar treatments with hypoeutectic irons (3.5–3.6 wt.% CE, 0.025 wt.% S, and 0.003 wt.% Al). A complex structure including primary graphite, austenite dendrites, and eutectic cells is obtained in hypereutectic irons, as the result of nonequilibrium solidification following the concept of a coexisting region. Dendrites appear to be distributed between eutectic cells at higher eutectic undercooling, while in inoculated irons and for lower undercooling, the eutectic cells are “reinforced” by eutectic austenite dendrites. A Zr, Ca, Al-FeSi alloy appears to be an effective inoculant in low S, low Al, gray cast irons, especially for a late inoculation technique, with beneficial effects on both graphite and austenite phases. First, inoculation influenced the nucleation of graphite/eutectic cell, and then their characteristics. A further role of these active elements directly contributed to form nucleation sites for austenite, as complex (Mn,X)S particles.

Keywords eutectic austenite dendrites, eutectic cell, graphite, hypereutectic gray irons, inoculation, metal matrix

1. Introduction

Thin-wall gray iron castings with <5 mm-wall thickness, are widely used in the automotive industry, for their many excellent properties including heat conductivity and vibration damping capacity. These important properties, in combination with reasonable strength, contribute to gray iron being the primary choice in the production of vital engine components for vehicles. Eutectic to slightly hypereutectic compositions (CE = 4.3–4.5 wt.%, carbon equivalent—CE) allow the best combination of castability, tensile strength, and thermal properties, especially for thin-wall gray iron castings (Fig. 1).

Superheated electric melted irons, at low S and very low Al contents, solidifying at high cooling rates, are more prone to free carbides and/or undercooled graphite formation. Superheating the iron in an induction furnace will lead to important changes in the iron not only to chemistry, but also to the liquid iron characteristics such as diffusion of elements and solution homogenization; remnant graphite dissolution; flotation of nonmetallic inclusions, especially large particles. After melting, the liquid metal may be considered to be in a colloidal state, which includes Fe-C-Si (Xi)-base solution; remnant graphite particles (0.1–1.0 μm) and nonmetallic inclusions. The liquid iron condition is heavily dependent on the quality of the charge materials but can be changed by superheating of the melt.

Liquid iron evolves from a colloidal liquid state after melting (suspension of graphite particles) through quasi-homogenous up to a quasi-ideal solution. Superheating is useful to sustain the dissolution of coarse remnant graphite, to float coarse inclusions and to de-activate the remnant microinclusions as un-controlled nuclei for graphite. Excessive superheating, however, will promote undercooled graphite morphologies and iron carbides.

Inoculation has a vital role to play in the continuing development of cast iron. FeSi containing 75–80 wt.% silicon became established as a basis for most common inoculants, although the need to control calcium and aluminum in a ferrosilicon inoculant was not fully understood and was far from satisfactory in the early days of inoculated gray iron production. More complex inoculants were developed and their enhanced performance was based on powerful oxide forming elements (some of which also form sulfides and nitrides) including Ca, Sr, Ba, Zr, Ce either individually or as a complex of two or three elements in FeSi-alloys (Ref 1).

The benefits of a late or in the mold inoculation technique for both gray and ductile irons are well known to foundrymen. Late additions in the mold are often used as a secondary inoculation step to prevent under-inoculation from inadequate ladle additions, fade, or malfunction of in-stream inoculation feeders. By inoculating at the last possible instance, control over microstructure and hardness values are easily achieved and inoculant fade is eliminated. Late inoculation eliminates the need for the dubious practice of super-inoculating to compensate for fade and allows for improved silicon control. Further, with the emphasis and continued growth of automatic mold pouring, difficulties associated with consistent stream inoculation are minimized. Finally, whether in-mold inoculation is being used as the primary mode of inoculation or as a secondary booster addition, overall inoculant addition rates for a given casting weight can be reduced.

The experimental investigation in this article was designed to monitor and characterize the structure of mold and ladle

Mihai Chisamera, Iulian Riposan, Stelian Stan, Cristina Militaru, and Irina Anton, Politehnica University of Bucharest, 313 Spl. Independentei, RO-060042 Bucharest, Romania; and Michael Barstow, Fremont, CA. Contact e-mail: riposan@foundry.pub.ro.

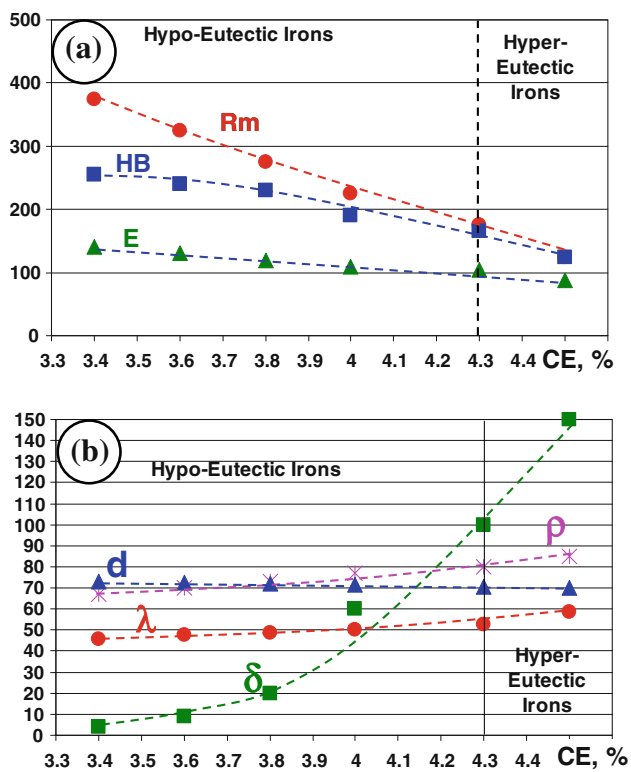


Fig. 1 Influence of CE on the mechanical (a) and physical (b) characteristics of gray cast irons (Rm: tensile strength, MPa; E: elastic modulus, GPa; HB: Brinell hardness; λ : thermal conductivity, W/m/k; d: density, $\text{g/cm}^3 \times 10$; ρ : electrical resistivity, $\Omega \text{ mm}^2/\text{m} \times 10^2$; δ : vibration damping capacity, 10^{-4})

inoculated, low-S (0.025 wt.% S), low-Al (0.003 wt.% Al), slightly hypereutectic (CE = 4.4-4.5 wt.%) electric melted gray irons, typical for high performance thin-wall castings. It describes the effect of a 0-0.25 wt.% Ca, Al, Zr-FeSi inoculant addition on structure characteristics, and compares to similar treatments with hypoeutectic irons (3.5-3.6 wt.% CE, 0.025 wt.% S, and 0.003 wt.% Al) (Ref 1-3).

2. Materials and Experimental Procedure

Experimental heats were induction melted in a graphite crucible (10 kg, 8000 Hz). Two base irons were considered, representing hypoeutectic and hypereutectic chemistries, 3.5-3.6 wt.% CE (3.02-3.05 wt.% C, 1.6-1.7 wt.% Si) and 4.4-4.5 wt.% CE (3.6-3.7 wt.% C, 2.4-2.5 wt.% Si), with 0.5-0.6 wt.% Mn, 0.11-0.13 wt.% P and 0.025 wt.% S in both irons (Ref 3). All of the iron melts are intentionally characterized by critical conditions for (Mn,X)S compounds formation to support graphite nucleation, using the control parameter $(\% \text{Mn}) \times (\% \text{S}) = 0.012-0.014$, which is less than the recommended range (0.03-0.06) (Ref 4), while $\text{Al} = 0.0026-0.0037\%$, is also less than the optimum range in hypoeutectic irons (0.005-0.010 wt.% Al) (Ref 5-10). Un-inoculated and inoculated irons were tested (green sand molds). A Zr, Ca, Al-FeSi inoculant (75 wt.% Si, 2.2 wt.% Ca, 1.5 wt.% Zr, and 1.2 wt.% Al) (Ref 11) was used at addition rates of 0.05-0.25 wt.% with a 0.2-0.7 mm particle size range.

In the first program, mold (M) inoculation was used. Experimental heats were superheated to 1500 °C and maintained at this level for 5 min. The test castings were all poured at 1430 °C. The specially designed test mold included a central downsprue, which delivered un-inoculated gray iron to a reaction chamber. Round test bar samples (20 mm diameter, 150 mm high) were gated off the inoculation reaction chamber. In the second program, successive ladle (L) inoculant additions were applied. Experimental heats were superheated to 1550 °C and tapped at 1470 °C. The same prescribed amount of inoculant was added as in the mold method, but in successive steps: 0.05 wt.% alloy was added in each step, to the previously treated iron, up to a total 0.25 wt.% of inoculant.

The effects of inoculation were analyzed by comparing the microstructures (carbides, eutectic shell, graphite, and metal matrix) of hypo- and hypereutectic irons treated with different amounts of the Ca, Zr, Al-FeSi alloy, with both inoculation techniques, using 20-mm diameter test bars. After casting, the bars were allowed to cool to room temperature before they were shaken out. The as-cast sample structure was analyzed in five areas at the mid-radius position, 50 mm from the end. In hypoeutectic irons, the graphite phase was observed to have two groups of flake graphite morphologies: particles resulting from higher eutectic undercooling were type D + E (undercooled graphite and interdendritic) with graphite nucleated at less eutectic undercooling, mainly as type A. Different structure analyses were performed on the samples: un-etched for graphite evaluation, 2% Nital etchant for carbides and ferrite/pearlite ratio, and CuCl_2 -base solution etchant for evaluation of eutectic cells and austenite dendrites.

Thermal analysis was conducted using Quik-Cups™ with a modulus of approximately 0.75 cm, equivalent to a 30-mm diameter bar. The cooling curve and its first derivative were recorded. The detailed procedure was presented in a previously published paper (Ref 3). Conventionally, eutectic undercooling is defined with reference to the start of the eutectic reaction (measured TEU) to the graphitic equilibrium eutectic temperature (calculated Tst), where $\Delta T_m = T_{st} - \text{TEU}$. The temperature of the end of solidification (measured TES), compared to the metastable (white) eutectic temperature (calculated Tmst) is illustrated by the parameter $\Delta T_3 = \text{TES} - \text{Tmst}$. Many individual elements have favorable or un-favorable influences on the Tst and/or Tmst level. Of these elements silicon has the most important influence in un-alloyed irons, especially where the trace element content is very low [$T_{st} = 1153 + 6.7 (\% \text{Si})$, $T_{mst} = 1147 - 12 (\% \text{Si})$] (Ref 1-3).

3. Results and Discussion

Hypereutectic gray irons present a specific structure (Fig. 2, 3). The graphite phase includes typical type C graphite morphology (Fig. 2a, b), but with different characteristics, depending on the type of inoculant, technique employed and addition rate. Compared to primary graphite, eutectic graphite has significantly more rotating twins and is more strongly branched.

3.1 Eutectic Structure

The gray iron crystal at the eutectic reaction stage is a grain of graphite plus austenite in a eutectic cell. The number and

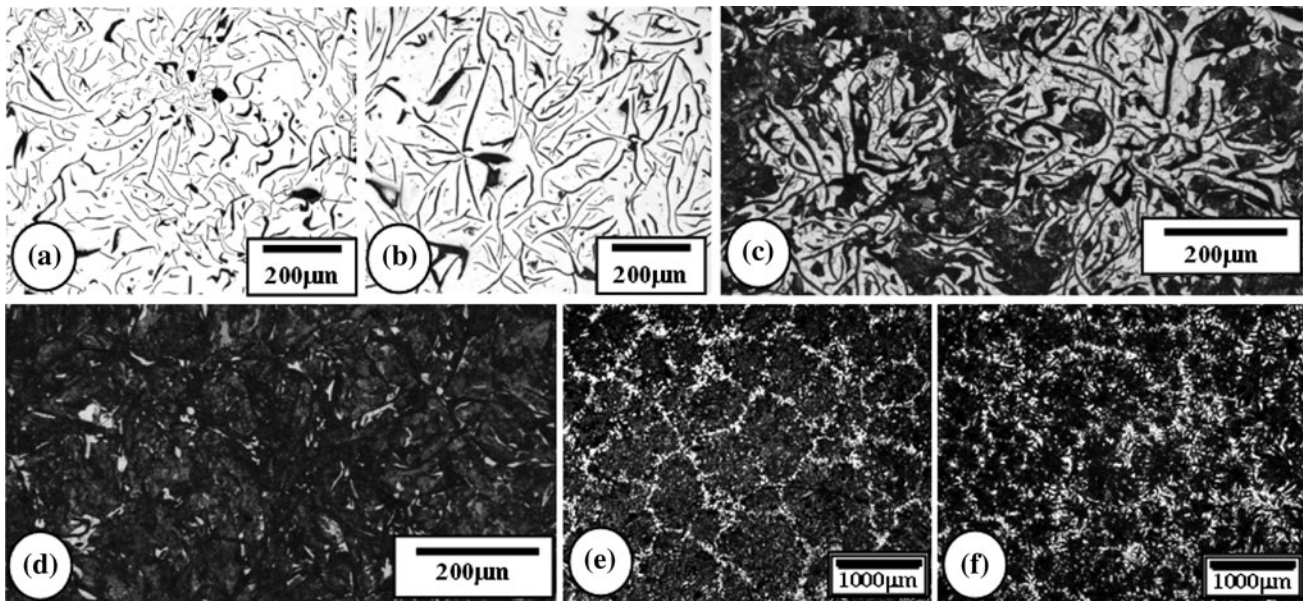


Fig. 2 Graphite (a, b), metal matrix (c, d), and eutectic cell (e, f) features of un-inoculated (a, c, e) and 0.15 wt.% in-mold inoculated (b, d, f), hypereutectic gray cast irons (a, b: unetched; c, d: Nital 2% etch; e, f: CuCl_2 -base solution etch)

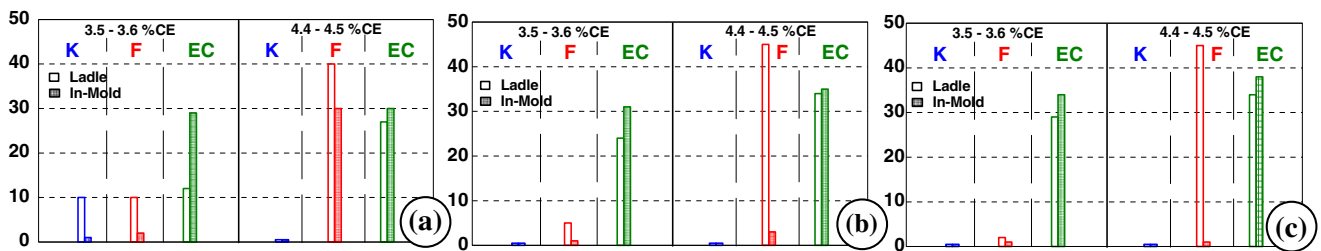


Fig. 3 Structure characteristics (K: carbides, %; F: ferrite, %; EC: eutectic cell count, cm^{-1}) of hypo- and hypereutectic, ladle and in-mold inoculated irons (a: 0.05 wt.%, b: 0.15 wt.%, and c: 0.25 wt.% alloy)

therefore size of the eutectic cells directly reflects the refinement of eutectic grains. As a general metallurgical rule, fine grains can increase the property of a metal. The characteristics of the eutectic cells of the experimental irons are influenced by iron chemistry but also by the inoculation employed. Graphite is the leading phase, while austenite precipitates between the graphite branches, making the solidification front of the eutectic grain almost spheroidal (Fig. 2e, f). In general, the number of eutectic cells reflects the number of nuclei for graphite formation in the eutectic iron melt. The chemical composition and nucleation state of the iron melt and ultimately the cooling rate during solidification appear to be major factors.

Carbon and silicon have important effects on the number of eutectic cells. The closer to the eutectic point the iron is, the greater the number of eutectic cells. The slightly hypereutectic composition led to a higher eutectic cell count compared to the relatively low hypoeutectic chemistries. Sulfur is another important element influencing eutectic cells. Low sulfur content is not beneficial for increasing the number of eutectic cells, since sulfides in the iron melt are an important component in graphite nuclei. Despite a Mn content of 0.5-0.6 wt.% in the irons being tested, a lower value of the control factor $\% \text{Mn} \times \% \text{S} < 0.02$ led to a low eutectic cell count in the base

iron, but eutectic cell count was also influenced by the inoculation parameters.

Inoculation is a process in which a small amount of substance is added into a melt to change its solidification characteristics by influencing the nucleation of the melt. For gray cast iron, the essence of inoculation is considered to be a process which influences the eutectic reaction in the iron melt. By adding an inoculant the nucleation of eutectic cells (grains), containing graphite and austenite, increases and improves graphitization, with the aim of reducing or eliminating carbide formation in thin-wall castings (reducing or preventing chill). Another objective is to reduce section sensitivity or the difference in structure between thin and thick-wall sections while promoting the formation of small and fine type A graphite. Overall, inoculation enhances the mechanical properties of cast irons and improves machinability.

Inoculation can greatly improve the nucleation state, thus increasing the number of eutectic cells (Fig. 3). The elements Al, Zr, and Ca introduced into iron by inoculation promote the formation of complex $(\text{Mn}, \text{X})\text{S}$ compounds, which feature in efficient flake graphite nucleation with less eutectic undercooling, in agreement with a three-stage graphite nucleation mechanism (Ref 5-9). In the first stage, Al and Zr participate in

an oxide compound formation, while Ca improved the graphite nucleation capability of MnS, which is nucleated on these original oxide sites, in a second stage (Fig. 4) (Ref 12).

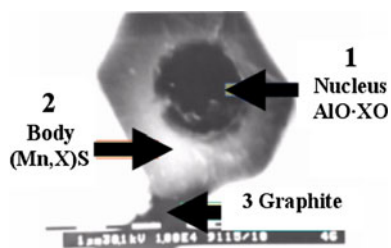


Fig. 4 Three stage model for the nucleation of graphite in gray cast iron

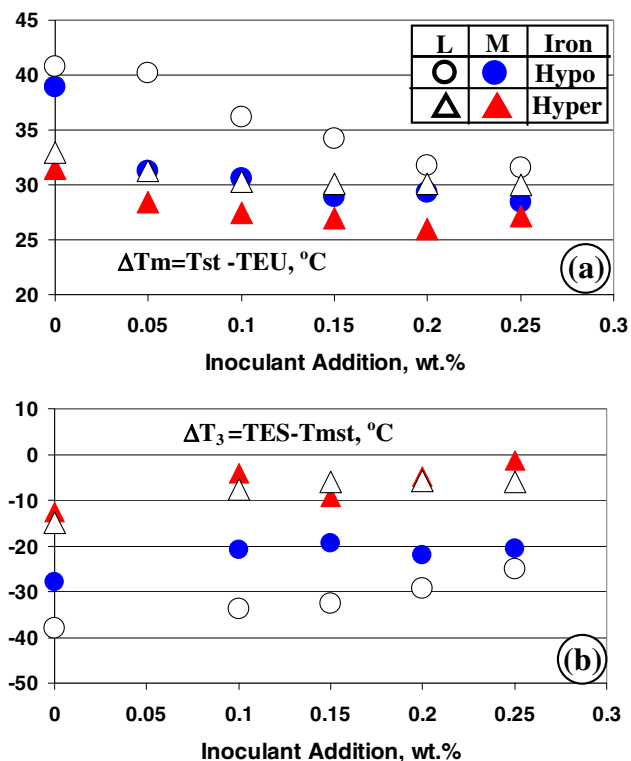


Fig. 5 Undercooling at start of the eutectic reaction (a) and at the end of solidification (b) of hypo- and hyper-eutectic, ladle (L) and in-mold (M) inoculated irons (Ref 3)

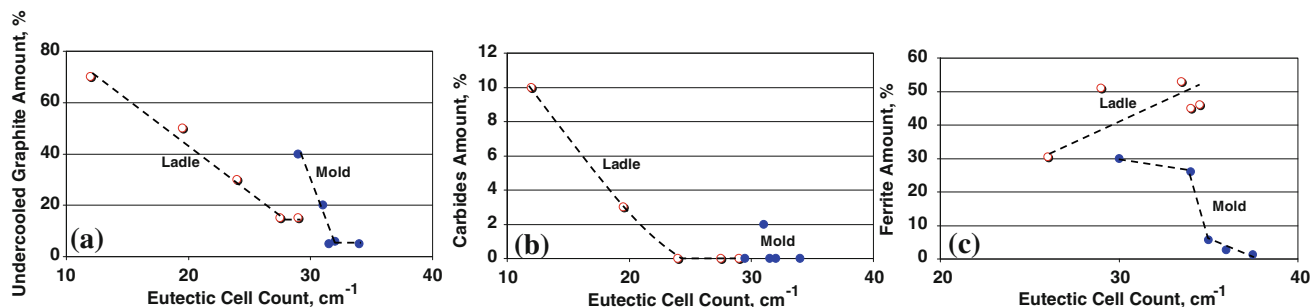


Fig. 6 Relationships between eutectic cell count and amount of undercooled graphite (a), free carbides (b), and ferrite (c) in ladle and mold inoculated hypo-eutectic (a, b) and hyper-eutectic (c) gray irons

Both inoculation technique and addition rate appear to be important factors. The higher graphitizing power of mold inoculation led to less eutectic undercooling, and favorable graphite morphologies, accompanied by a higher eutectic cell count. The smallest eutectic cell size (<300 μm size) was obtained with mold inoculation of hypereutectic melts, with <27 °C eutectic undercooling (ΔT_m) [relative to the stable eutectic temperature] and the least undercooling at the end of solidification (ΔT_3), with reference to the metastable eutectic temperature (Fig. 5) (Ref 3).

Eutectic cell count appears to be an important parameter of the microstructure, in both hypo- and hypereutectic gray irons. A finer eutectic structure in inoculated irons, either described as smaller size or high cell count, typically favors lower amounts of undercooled graphite and free carbides in hypoeutectic irons (Fig. 6 a,b), when in the mold inoculation is employed.

3.2 Metal Matrix

If free carbides are successfully avoided, the performance of the metal matrix depends on the graphite morphology and other inoculation effects. Mold inoculation resulted in improved graphite particle characteristics and consequently limited any extensive carbon diffusion during the eutectoid transformation. As a result, a lower amount of ferrite was obtained in an iron, which already had had a 0.15 wt.% inoculant addition, resulting in more than 97% pearlite (Fig. 2d). Despite the hypereutectic chemistry, the base iron matrix is comparable to that of a hypoeutectic iron. Increasing the inoculant addition rate has an important positive influence, especially in the lower addition range with the mold inoculation technique.

In the production of high performance, slightly hypereutectic iron, inoculation was found to promote high eutectic cell count, with favorable graphite morphologies and, consequently, an increased amount of pearlite, alternatively less ferrite (Fig. 6c).

This experimental program shows the advantages of appropriate inoculant selection (Zr, Ca, Al-FeSi alloy) for thin-wall casting iron melted in the new generation of high performance coreless induction furnaces (200-1000 Hz, >250 kW/ton) with lower sulfur and aluminum contents. In general, the efficiency of 0.05-0.15 wt.% inoculation in the mold is comparable to or better than 0.15-0.25 wt.% inoculation in the ladle.

3.3 Austenite Dendrites

It is generally agreed that proeutectic austenite grows dendritically in hypoeutectic cast irons. The parameters describing austenite characteristics include secondary dendrite

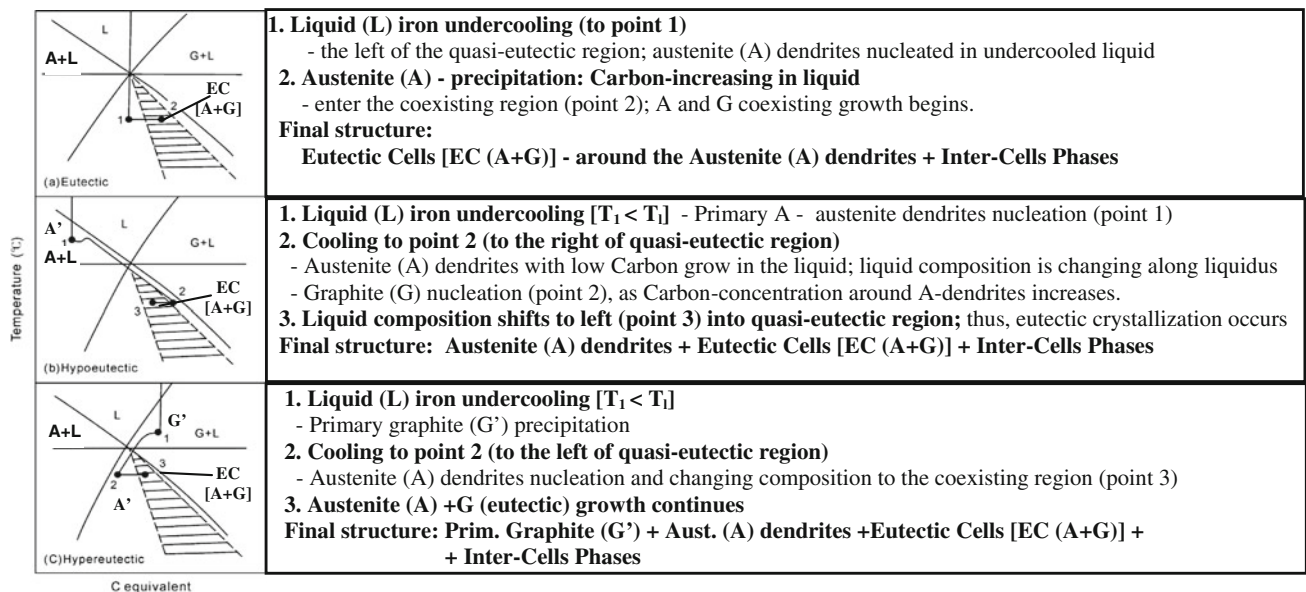


Fig. 7 Nonequilibrium solidification process of commercial cast irons

arm spacing, average arm length, amount of dendrites, and orientation. Among these, the amount of dendrites is a predominant factor. This is different from other alloy materials; the predominant factor controlling cast iron strength is the amount of austenite, rather than secondary dendrite arm spacing. The influence of dendrites on the mechanical properties of gray iron is similar to the reinforced steel bars effect in concrete or fibers in composites acting as a support frame. The greater the dendrite amount, the stronger the cast iron is. The influence of secondary axis spacing on cast iron properties is not as significant as that of the dendrite amount; nevertheless, with decreased secondary axis spacing, the tensile strength also increases and this trend is decreased with increasing CE. If dendrites are present as short, small isolated forms in a cast iron structure, an improvement in tensile strength is not significant. When dendrites cross each other and form networks, the area of interaction is increased, which is more significant for strength improvement (Ref 13).

The most broadly accepted explanation of the eutectic solidification of gray cast iron states that eutectic units are formed by nearly spherical aggregates of austenite and graphite growing cooperatively, with both phases in contact with the melt, producing so-called “eutectic cells.” However, it was found that the solidification of eutectic and hypereutectic cast irons also involves austenite dendrites (Ref 14). Regardless of CE, commercial gray irons show a similar macrostructure, as a quasi-eutectic structure and a direct result of undercooling, with eutectic solidification dominated by large austenite dendrites. As dendrites grow, they contact each other, defining the grain structure in hypereutectic irons.

Industrially processed irons contain substantial impurities and trace elements, with a very complicated state of nucleation in the melt. In addition, the cooling rate during casting solidification is fast, compared to the very slow equilibrium phase diagram cooling rates (0.008-0.04 °C/s) for a very pure vacuum melted material (Ref 15).

According to the concept of a coexisting region and nonequilibrium solidification of gray iron castings (Ref 15),

the final structure of eutectic and hypereutectic gray irons is different compared to equilibrium phase diagram results, mainly due to the presence of dendritic austenite (Fig. 7). As a result, in hypereutectic irons, a complex structure including primary graphite, dendritic austenite, and eutectic cells (austenite + graphite) is obtained.

Figure 8 and 9 shows the real structure of 4.4-4.5 wt.% CE gray irons, solidified in 20-mm diameter samples (CM = 0.50 cm), at a cooling rate $CR = 1.5^\circ\text{C/s}$ during solidification. The crystallization conditions are significantly different from the special conditions required to generate an equilibrium phase diagram, measured under special conditions. As a result, nonequilibrium solidification, following the concept of a coexisting region was recorded.

Typical austenite dendrite morphology, with a long primary crystal axis and obvious secondary axis dendrites, characterize the structures (Fig. 8a, b, 9a), despite the slightly hypereutectic region. A high CE for these irons lowered the amount, and length, of the austenite dendrites.

In general, inoculation decreases undercooling, and therefore, reduces the dendrite amount. The presence of eutectic austenite dendrites is more evident in un-inoculated irons (Fig. 8a, 9a), or at lower inoculant addition rates (Fig. 8b), especially for ladle-treated irons (Fig. 8). Since higher eutectic undercooling prevailed after ladle inoculation, in comparison to mold inoculation (Fig. 6), dendritic austenite is more visible in these irons (Fig. 8).

Eutectic austenite dendrites and eutectic cells grow differently, depending on the solidification conditions. The distribution, morphology, and orientation of austenite dendrites are closely related to the level of eutectic undercooling. In un-inoculated irons or at low inoculant additions the eutectic austenite dendrites are mainly distributed between eutectic cells (Fig. 8a, b, 9a). However, in inoculated irons, the higher numbers of eutectic cells are “reinforced” by austenite dendrites, as shown in Fig. 8c-f and 9b-d.

After graphite precipitates, austenite forms on the lateral side of the graphite flakes. The difference in atom spacing on

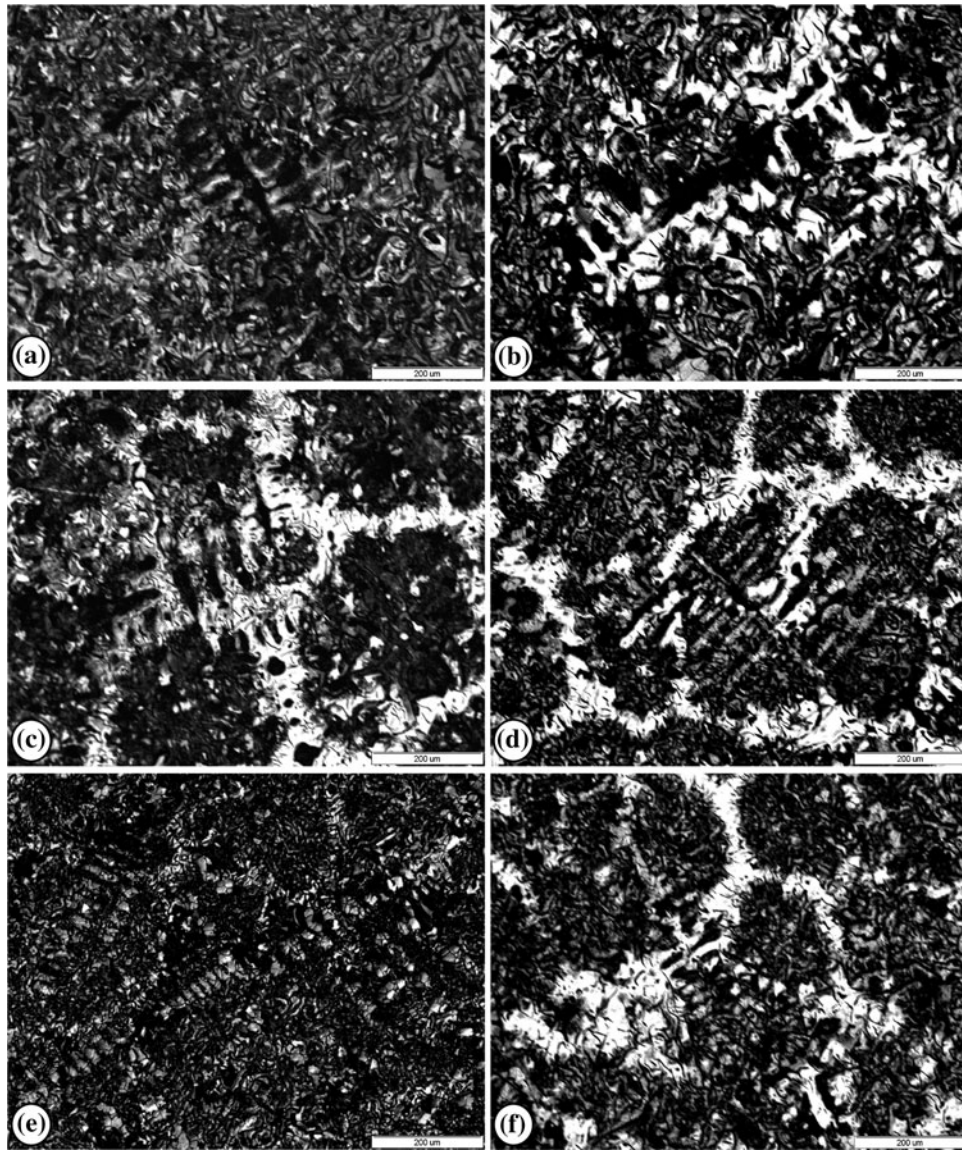


Fig. 8 Dendritic structure in ladle-inoculated, 4.4-4.5 wt.% CE gray cast irons (a: un-inoculated, b: 0.05 wt.%, c: 0.10 wt.%, d: 0.15 wt.%, e: 0.20 wt.%, f: 0.25 wt.% alloy) (CuCl_2 -base solution etch)

the (0001) plane of graphite, and on the (111) plane of austenite, is 2.3% (Ref 15, 16); the lattice mismatch, δ , between the two phases is very small at only 4.55% (Ref 15, 17). Hence, with graphite as the substrate, and attaching to the lateral plane (0001) of graphite, austenite quickly nucleates and grows in the form of dendrites (Ref 15). The growth of austenite along the plane (0001) of graphite is influenced by conditions during crystallization.

Residual elements in the base iron and/or from inoculation can also influence the characteristics of the austenite dendrites, by directly influencing the nucleation and growth of austenite. Al, Zr, Ti, V, Cr, Mo, Ce, B, and Bi can increase the dendrite amount, especially by forming substrates for austenite, while inoculating with a Ca and Ba containing FeSi alloy, shortens the dendrite length and decreases the dendrite amount (Ref 15, 18).

It is expected that the use of conventional inoculation (Zr, Ca, Al-FeSi alloy) to control graphite also directly or indirectly

influenced the eutectic austenite nucleation and growth, in addition to dendritic austenite. Initially, inoculation influenced the nucleation of graphite and then its characteristics. A further role of these active elements directly contributes to forming nucleation sites for austenite, as complex (Mn,X)S particles.

4. Conclusions

- The solidification structure of gray irons at different CE levels is controlled to a more acceptable level, if these irons are inoculated with a performance technique, such as an addition to the mold. A higher inoculant addition rate led to better graphite morphologies and a higher eutectic cell count.
- Finer eutectic structures in inoculated irons, as small-sized grains or higher cell count favor lower amounts of under-cooled graphite, and free carbides, in hypoeutectic irons,

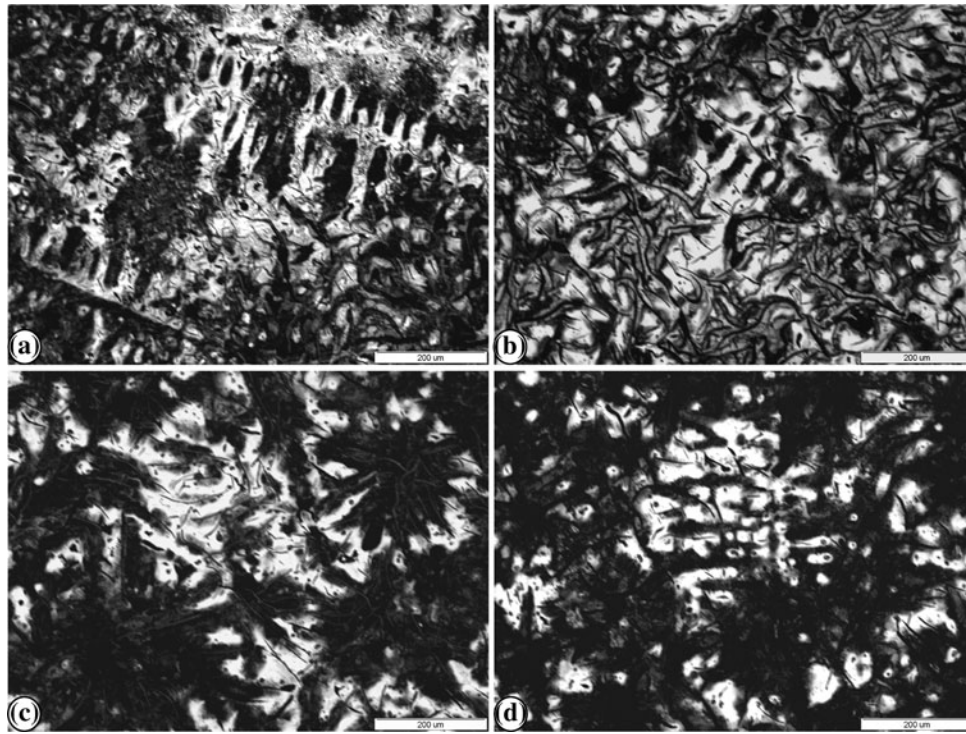


Fig. 9 Dendritic structure in mold-inoculated, 4.4-4.5 wt.% CE gray cast irons (a: un-inoculated, b: 0.05 wt.%, c: 0.15 wt.%, d: 0.25 wt.% alloy) (CuCl₂-base solution etch)

and less ferrite in hypereutectic irons, especially with the performance of in-mold inoculation;

- In general, the efficiency of 0.05-0.15 wt.% alloy for mold inoculation is comparable to or better than 0.15-0.25 wt.% ladle inoculation additions;
- A complex structure including primary graphite, dendritic austenite, and eutectic cells (austenite + graphite) is obtained in hypereutectic irons, as the result of nonequilibrium solidification following the concept of a coexisting region.
- Eutectic austenite dendrites and eutectic cells grow differently, depending on the solidification conditions. The distribution, morphology, and orientation of austenite dendrites are closely related to the level of eutectic undercooling.
- The presence of eutectic austenite dendrites is more evident in un-inoculated irons or at lower inoculant additions, especially for ladle-treated irons, at higher eutectic undercooling. In these irons, the dendrites are mainly distributed between eutectic cells.
- In inoculated irons and irons with lower undercooling, higher numbers of eutectic cells are “reinforced” by austenite dendrites.
- A Zr, Ca, Al-FeSi alloy appears to be an effective inoculant in low S, low Al, gray cast irons, especially for a late inoculation technique, with beneficial effects on both graphite and austenite phases. Initially, inoculation influenced the nucleation of graphite/eutectic cell, and then their characteristics. A further role of these active elements directly contributes to forming nucleation sites for austenite, as complex (Mn,X)S particles.

References

1. M. Chisamera, S. Stan, I. Riposan, G. Costache, and M. Barstow, Solidification Pattern of In-Mold and Ladle Inoculated Low Sulfur Hypoeutectic Gray Irons, *AFS Trans.*, 2008, **116**, p 641–652
2. M. Chisamera, I. Riposan, S. Stan, E. Stefan, and G. Costache, Thermal Analysis Control of In-Mould and Ladle Inoculated Grey Cast Irons, *China Foundry*, 2009, **6**(2), p 145–151
3. I. Riposan, M. Chisamera, S. Stan, G. Costache, and M. Barstow, A Comparison of Mould and Ladle Inoculation Treatments of Low S Hyper-and-Hypoeutectic Grey Cast Irons, *Proceedings of the 69th World Foundry Congress*, Hangzhou, China, WFO/FICMES, 2010, p 342–351
4. R. Gundlach, Observations on Structure Control to Improve the Properties of Cast Irons, The Honorary Cast Iron Lecture, *AFS Metalcasting Congress*, Atlanta, USA, 2008, Paper 08-158
5. I. Riposan, M. Chisamera, S. Stan, and T. Skaland, The Key Role of Residual Al in Chill Tendency and Structure Characteristics of Un-Inoculated and Ca/Sr Inoculated Grey Irons, *66th World Foundry Congress*, Istanbul, Turkey, 2004, p 775–790
6. M. Chisamera, I. Riposan, S. Stan, and T. Skaland, Investigation of Effect of Residual Al on Solidification Characteristics of Un-Inoculated and Ca/Sr Inoculated Gray Irons, *AFS Trans.*, 2004, **112**, p 867–877
7. I. Riposan, M. Chisamera, S. Stan, P. Toboc, C. Ecob, and G. Grasmio, High Efficiency Preconditioning of Electrically Melted Grey Cast Irons, *68th World Foundry Congress*, Chennai, India, 2008, Paper 53
8. I. Riposan, M. Chisamera, S. Stan, C. Ecob, and D. Wilkinson, Role of Al, Ti, and Zr in Gray Iron Preconditioning/Inoculation, *J. Mater. Eng. Perform.*, 2009, **18**(1), p 83–87
9. I. Riposan, M. Chisamera, S. Stan, C. Hartung, and D. White, Three-Stage Model for the Nucleation of Graphite in Grey Cast Iron, *Mater. Sci. Technol.*, 2010, **26**(12), p 1439–1447
10. I. Riposan, M. Chisamera, S. Stan, and D. White, Complex (Mn, X)S Compounds—Major Sites For Graphite Nucleation in Grey Cast Iron, *China Foundry*, 2009, **6**(4), p 352–358
11. ZIRCINOC Inoculant-Product Data Sheet, ELKEM Foundry Prod., 2007. www.foundry.elkem.com

12. I. Riposan, M. Chisamera, S. Stan, and T. Skaland, Graphite Nucleants (Microinclusions) Characterization in Ca/Sr Inoculated Grey Irons, SPCI 7—Science and Proc. of Cast Iron Int. Conf., Barcelona, Spain, 2002, *Int. J. Cast Metal Res.*, 2003, **16**(1–3), p 105–111
13. Z. Jiyang, Colour Metallography of Cast Iron, *China Foundry*, 2009, **6**(3), p 255–267
14. G. Rivera, P.R. Calvillo, R. Boeri, Y. Houbaert, and J. Sikora, Examination of the Solidification Macrostructure of Spheroidal and Flake Graphite Cast Irons Using DAAS and ESDD, *Mater. Charact.*, 2008, **59**, p 1342–1348
15. Z. Jiyang, Colour Metallography of Cast Iron, *China Foundry*, 2009, **6**(1), p 57–69
16. X. Chen, Growth Mechanism of Spheroidal Graphite in Primary Crystallization of Cast Iron (Edited by Foundry Division, Harbin Institute of Technology), Harbin Institute of Technology Press, Harbin, China, 1978 (in Chinese)
17. T. Mizoguchi, J.H. Perepezko, and C. Loper, Jr., Nucleation During Solidification of Cast Irons, *AFS Trans.*, 1997, **105**, p 89–94
18. G.F. Ruff and J.F. Wallace, Control of Graphite Structure and Its Effect on Mechanical Properties of Grey Iron, *AFS Trans.*, 1976, **84**, p 705–728